

**Membrane phase dependent occlusion of intramolecular GLUT1
cavities demonstrated by atomistic simulations**

JI-F, PJQ, RJ, and CD

Abstract

Experimental evidence has shown a close correlation between the composition and physical state of the membrane bilayer and glucose transport activity via the glucose transporter GLUT1. Cooling alters the membrane lipid from fluid to gel phase and also causes a large decrease in net glucose transport rate. Here, molecular dynamics simulations are used to investigate how the physical phase of the membrane alters glucose transporter structural dynamics. Simulations from an initial fluid to gel phase reduces the size of the cavities and tunnels traversing the protein connecting the external regions of the transporter and the central binding site. These effects can be ascribed solely to membrane structural changes since *in silico* cooling of the membrane alone, whilst maintaining the higher protein temperature, shows very similar protein structural and dynamic changes to those with uniform cooling. These results demonstrate that the protein structure is sensitive to the membrane phase and has implications on how transmembrane protein structures are responsive to their physical environment.

Keywords: Molecular dynamics simulations; glucose transport; transporters; phase transition

Introduction

Glucose transporters (GLUTs), belonging to the sugar transporter branch SLC2A of the Major Facilitator Superfamily (MFS) (1), are essential membrane proteins in eukaryote cell metabolism and are thus, the focus of numerous functional, structural and drug discovery studies. The human GLUTs display organ and membrane specific distributions with distinct kinetics and substrate specificities (2). With the exception of the myo-inositol/H⁺ symporter GLUT13, all GLUTs are uniporters that facilitate monosaccharide passive downhill diffusion (3, 4). The glucose transporters share an identical structural fold comprising 12 transmembrane helices (TM1-TM12), which have a binding site located in the central region of the transporter delineated by residues contributed from both N- and C- domains. A substantial endofacial cytosolic linker joins the N and C domains that may play a role in the transport function by securing the closure of the inward gate (5).

The glucose transport mechanism of GLUT1 has been studied using biochemical and molecular biology methods, including scanning mutagenesis, fluorescence resonance energy transfer (FRET), and computational approaches that include molecular dynamics simulations (6-10). Data from most of these studies and recent crystal structures of the GLUT family (11-13) support a mechanism in which a binding site for glucose is alternatively accessible from either side of the membrane, involving movements of the N- and C-domains over a rotation axis located at the central binding site and perpendicular to the bilayer plane; this is the so-called 'alternating access mechanism'. However, crystallographic structures of several occluded conformations of the transporter (13), both inward- and outward-facing, suggest an alternative transport mechanism that relies on the adaptation of the protein to its environment (14). In addition, the endofacial domain is thought to undergo a substantial conformational change during the transport cycle, implying a role as a 'gate' at the intracellular side (13).

An alternative model for sugar transport, the so-called 'multisite model' has been proposed, based on cytochalasin-B inhibitor binding studies (8), docking studies (15-17) and molecular dynamics simulations (18). According to this model, ligands can diffuse between multiple adjacent sites within a branched network of transiently

open tunnels and cavities spanning the transporter. These transient openings within the intramolecular tunnels are triggered by small-scale changes in the carbon skeleton and side groups or reptations, widening the tunnel bottlenecks without the requirement of any global structural rearrangements.

Membrane hydrophobic thickness changes have previously been shown to act as a trigger for bacterial cold sensor *Bacillus subtilis* DesK. At cold temperatures this acts as a kinase to autophosphorylate a histidine residue. The phosphoryl residue is transferred to an aspartate in the DNA-binding response regulator. This leads to activation of an acyl lipid desaturase which desaturates and fluidizes the membrane lipids, thereby returning the membrane to the fluid state (19). This mechanism has been called the “sunken buoy” motif (20).

The transport properties of GLUT1 embedded in liposomes, have been experimentally evaluated as a function of the composition and structural features of the lipid bilayer (21, 22). These studies concluded that although short-chain lipids were able to support glucose transport activity in the gel phase, transport dramatically increased in the membrane fluid state (23). As an example, with 1,2-dipalmitoyl-sn-glycero-3-phosphocholine (DPPC) membranes, transport activity vanishes during cooling to the gel phase but is increased during pre-melt and phase transition and recovered fully in the fluid phase. However, in the gel phase inclusion of 20% cholesterol into DPPC membranes activated transport, although a larger cholesterol enrichment inhibits transport (24). It has been proposed that the cholesterol-dependent increase in transport is largely due to an decrease in membrane microviscosity. The slowing of transport at higher cholesterol concentrations may be due to inhibitor complexes formed with the transporter. The complex role of cholesterol between membrane lipid structure and transporter function is still unresolved.

Here, molecular dynamics (MD) simulations have been employed to investigate at the atomistic level whether the structural changes and interaction patterns of the bilayer phase contribute to structural modifications in the glucose transporter. Small scale correlated movements of the C α backbone atoms and sidechains of GLUT1 controlled by the physical state of the membrane, are found to direct the passage of

glucose, as assessed by in silico docking methods. The gel membrane phase particularly alters the cavity structures. Additionally, the extra-membranous loop regions of the transporter, independent of any membrane constraints, are subject to large structural changes and therefore, are likely gating sites for ligand entry into transmembranous domains.

Materials and Methods

System Setup

The crystal structure of the human glucose transporter (GLUT1, PDB ID: 4PYP) (11) was used as a starting point for the computational work. The structure was resolved in an inward-open conformation, with a glucose-derivative bound to the main binding site. For the purpose of the simulations, the crystallographic sugar-derivative was not included in the model. The initial GLUT1/DPPC system was generated using the Membrane Builder module (25) with default options in the CHARMM-GUI website (26). Initially, a membrane patch of 100 Å x 100 Å DPPC lipids was built. The membrane contained 205 molecules of 1, 2-dipalmitoyl-*sn*-glycero-3-phosphocholine (DPPC). This choice was based on a compromise between size and computational resources. Subsequently, the GLUT1 structure was inserted into the membrane patch. To avoid steric clashes, lipids in close contact with the protein were deleted. This resulted in an asymmetric lipid distribution with 100 lipid molecules in the cytoplasmic leaflet and 105 lipid molecules in the external leaflet. The combined system was then solvated and neutralized to produce a rectangular simulation box of dimensions 96 x 96 x 108 Å³ and ~80,000 atoms. Two independent simulations were run at different temperatures: one above (323.15 °K) and one below (308.15 °K) the DPPC phase transition temperature of 314.15 °K.

Molecular Dynamics Simulations

The software NAMD2.9 was employed to perform the molecular dynamics simulations (27). The CHARMM36 force field was used to model the protein and lipids (28). Standard CHARMM parameters were used for ions (29), and the TIP3P model for water (30). Pressure was maintained at 1 atm by a Langevin piston (31), with a damping time constant of 50 ps and a period of 200 ps. A semi-isotropic

pressure coupling method was used in all the simulations. For the NAMD calculations, the pressure of the piston acted independently in each dimension, but maintained a constant ratio in the x,y axis, corresponding to the plane of the membrane. The temperature was maintained constant by coupling the system to a Langevin thermostat, with a damping coefficient of 1 ps^{-1} . The particle mesh Ewald (PME) algorithm was used for the evaluation of electrostatic interactions beyond 12 Å, with a PME grid spacing of 1 Å, and NAMD defaults for spline and κ values (32). A cut-off at 12 Å was applied to non-bonded forces. Both electrostatics and van der Waals forces were smoothly switched off between the switching distance of 10 Å and the cut-off distance of 12 Å, using the default switching function in NAMD. A Verlet neighbor list with pair-list distance of 13.5 Å was used to evaluate non-bonded neighboring forces within the pair-list distance (33). The lengths of covalent bonds involving hydrogen atoms were constrained by the SETTLE algorithm (34, 35) in order to use a 2-fs time-step. The multi-time step algorithm Verlet-I/r-RESPA (33, 35) was used to integrate the equations of motion. Both systems were subject to 10,000 steps of energy minimization, followed by an equilibration consisting of sequential release of various restraints added to the system (26): (i) harmonic restraints to heavy atoms of the protein and ions, (ii) repulsive restraints to prevent water from entering in the hydrophobic region of the membrane, and (iii) planar restraints to hold the position of the lipid headgroups along the z-axis. Subsequently, 400-ns production runs were executed at each temperature.

To ensure that temperature effects are ascribed exclusively to the phase state of the membrane, two additional simulations where the protein and bilayer were held at two different temperatures were performed with the GROMACS 5.0 software package (36) (Figure S1). In the first simulation, the temperature of the bilayer was set at 323.15 °K to be in the fluid phase, whilst the temperature of the protein was set at 308.15 °K, below the bilayer phase transition. In contrast, in the second simulation, the temperature of the protein was set at 323.15 °K whilst embedded in a gel DPPC membrane at 308.15 °K. Each system was simulated for 400 ns using identical equilibration and production protocols as the ones described earlier.

Analysis of the MD trajectories

The program CAVER 3.0 (37) was used to analyze the size and shape of the available pathways for glucose transit from the GLUT1 inward (IN) and outward (OUT) faces to the glucose binding site (GBP) at the center of the protein (Figure 1B). Aligned coordinate files from the trajectories spaced at 1 ns were selected. The algorithm works by constructing a Voronoi diagram to describe the skeleton of the water channels within the framework of the protein structure, followed by a cluster analysis of all the channels identified. For this study, a spherical probe of 0.8 Å radius was selected with a weighting coefficient of 1, clustering threshold of 12, shell radius of 18 Å and shell depth of 4 Å. The starting point for the calculation was chosen at the center of mass of residues I168, Q282, Q283, N288 and E380 of GLUT1, according to the glucose derivative - protein interactions present in the GLUT1 X-ray structure (PDB ID: 4PYP) (11).

The membrane thickness was calculated using the MEMBPLUGIN analysis tool in VMD (38).

The numbers of water molecules along the z-axis of the central channel in the gel and fluid phases were digitized using Imagej profiling into 1320 bins representing average numbers per 300 ps per bin. The plots were sub-divided into 8 5 Å strips. The water molecules in each bin were cross-correlated between $n = 1$ to 8. Contour maps of the matrices of the regression coefficients R_{ij} was constructed for the water molecules in the simulations with the bilayer in the gel and fluid phases.

Docking calculations

Glucose was docked into the GLUT1 transporter *via* a Lamarckian genetic search algorithm as implemented in the AutoDock 4.2 software package (39). Docking calculations were performed for representative snapshots of the simulations of the transporter embedded in the fluid and gel phases. Ten different snapshots were extracted from the last 100 ns of each simulation, and 100 AutoDock runs were performed for each of the structures. A grid with dimensions of $80 \times 80 \times 120 \text{ Å}^3$ centered on the glucose binding site was used, with binding modes ranked by a scoring function implemented in the Autodock software. Gasteiger atom charges were assigned to the protein and glucose atoms using AutoDock tools.

Results and Discussion

For each simulation, the carbon backbone root-mean-square deviation (RMSD) was calculated relative to the initial crystallographic structure (Figure S2). In both simulations, the RMSD values were computed for the 400-ns production trajectories taking as a reference the initial X-ray structure. At least 100 ns were needed for the RMSD to plateau. Converge to a specific value within the resolution of the initial X-ray structure (3.17 Å) suggests that the protein structures remain relatively stable despite of removal of the glucose derivative from the crystal structure that may have influenced the stability of the protein. The RMSD values of the fluid phase system reflect larger structural changes corresponding to movements of the endofacial loops located at the cytoplasmic leaflet. After approximately 60 ns, a plateau was reached in the simulation of the gel phase of ~2.5 Å. A structural comparison of the glucose binding site in the GLUT1 X-ray structure and in the gel/fluid MD trajectories where glucose was absent from the active site, results in small changes in the surrounding residues, in particular Asn288, which flips to interact with another neighbour residue (Figure S3).

Glucose does not readily permeate phospholipid bilayers as demonstrated by its osmotic activity, and thus, the potential pathways available for glucose to navigate through the transporter were explored when embedded in a lipid bilayer, either in fluid or gel phase. Searches for cavities were computed using the respective MD trajectories. Two main pathways connecting the center of the protein with the endo- and exofacial environments of the membrane were identified (Figure 1A). In addition, other cavities connecting the central binding site with the exterior of the membrane were detected. However, these were relatively narrow and observed much less frequently during the simulations than the main inward and outward glucose entry routes. Therefore, it is unlikely that these secondary routes offer viable pathways for glucose entry and release, and hence, they were disregarded.

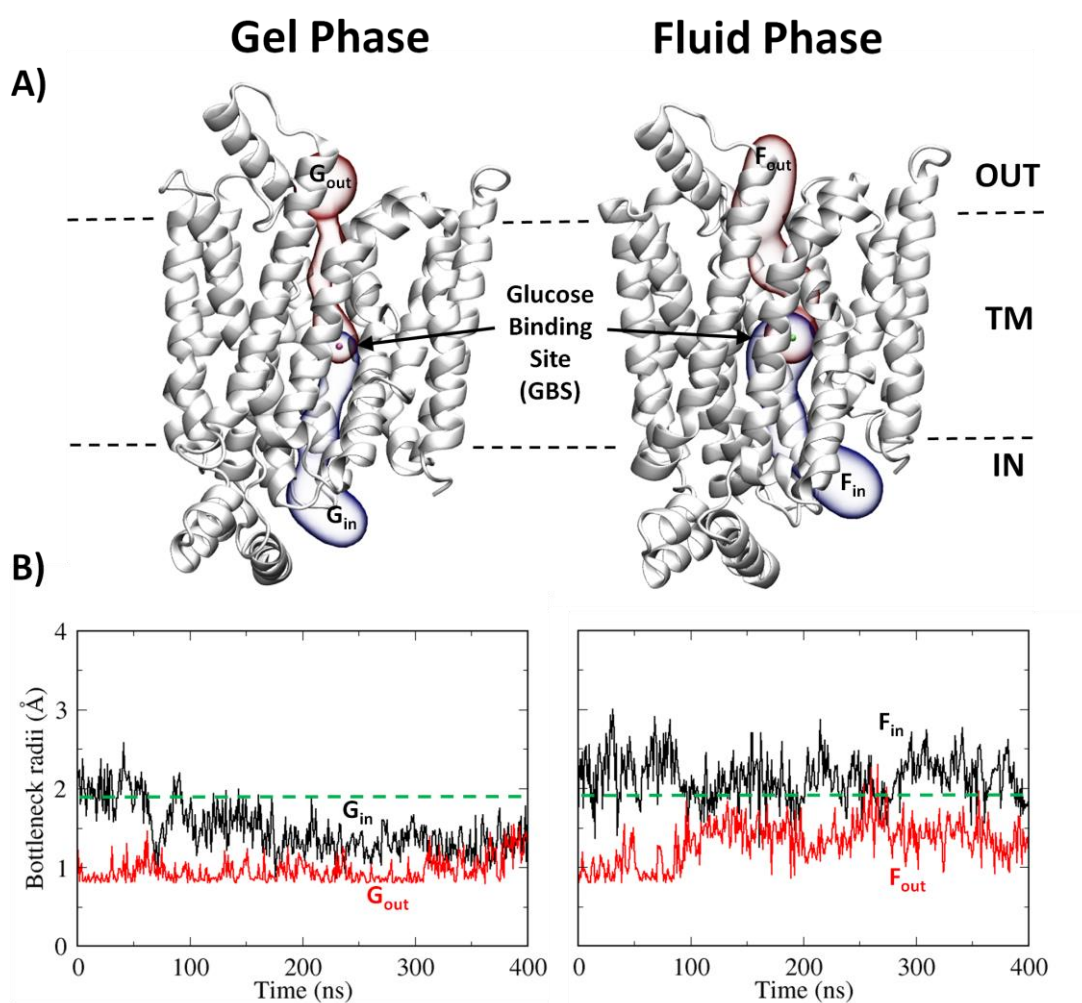


Figure 1. (A) Schematic representation of the glucose pathway in the protein that extends from the intracellular (IN) to extracellular (OUT) sides of the membrane through the main glucose binding site (GBS) at the center of the transporter. The permeation pathway connecting the intracellular part up to the main glucose binding site is shown in blue, and labeled with the subscript 'in'. The pathway connecting the extracellular side with the main glucose binding site is shown in red and labeled with the subscript 'out'. G and F refer to the gel or fluid phases of the membrane, respectively. (B) Evolution of the bottleneck radius of the main cavity running along the transporter with time in each membrane phase. The green discontinuous line indicates the minimal radius of a glucose molecule.

The average and maximum bottleneck radii of the inner and outer (IN and OUT) permeation branches of the main permeation pathway in the gel and fluid simulations were computed and are reported in Table S2. The values found highlight the effects of the physical phase of the bilayer. The dimensions of the pathway

available for glucose to access the central binding site, from either side of the membrane, are reduced when the protein is embedded in a membrane in gel phase as opposed to fluid phase. The maximum value of the bottleneck radius found in the inward-facing branch of the pathway, either in the gel or fluid phases (G_{in} or F_{in}), is wide enough to allow the passage of glucose molecules with a minimal radius of 1.9 Å (40, 41). When the membrane is in the gel phase, the maximum radius of the outer gate was found to be 1.54 Å, smaller than the minimal glucose radius. Therefore, when the membrane is in the gel phase, glucose can only gain access to the central binding site via the endofacial branch of the pathway, whereas in the outward-facing route, glucose translocation is only possible in the fluid phase.

Analysis of the time course of the bottleneck radii during the 400-ns MD simulations highlights the larger effect of the gel bilayer on the transporter structure in the context of glucose translocation (Figure 1B). The outward-facing branch of the pathway has a bottleneck radius close to the minimal radius of 0.8 Å used for the search of cavities, with a maximal 0.5 Å deviation from this value. In contrast, the inward pathway evolves from an open state with a bottleneck radius greater than the 1.9 Å minimal glucose radius. However, the tunnel structure becomes progressively narrower until complete closure occurs at ~180 ns of MD simulation. When the fluid membrane is considered, the bottleneck radius of the inward branch of the pathway is generally wider and more stable, having values exceeding the minimum glucose radii for almost the entire simulation. In contrast, the outward branch of the pathway is accessible only during short time periods for example from 270 to 285 ns (Figure 1B).

Therefore, in the gel state, glucose is inaccessible to the central binding site because both, inward and outward branches are too narrow. Crucially however, in the fluid phase, glucose can occasionally gain access to the inner parts of the transporter from the external solution. Since access through the inward branch of the pathway is almost continuously open, it is evident when the membrane is in the fluid state that opening of the outward branch is the main rate factor limiting glucose transit.

To gain additional appreciation regarding the frequency that these bottlenecks attain sufficient width to permit glucose exchange, only time intervals with a

bottleneck radius smaller than the minimal glucose radius of 1.9 Å were analyzed (Figure S4). The inward branch of the pathway, when embedded in a fluid bilayer, spontaneously opens and closes to glucose access with a maximum open interval of almost 50 ns. In contrast, the outward-facing branch of the pathway for the majority of time remains closed although it widens for short intervals. These observations validate the 'multisite model' for sugar transport (42-44) in which glucose molecules can transit along a network of moderately high affinity binding sites in the absence of large scale global rearrangements of the protein structure, i.e. without any alternating access contribution. Another recent computational study of the GLUT1 glucose transport also supports a combination of the multisite model and the classical alternating access mechanistic model as the key determinants for sugar translocation (45).

Representative heat maps of the time-dependent evolution of the radius of pathway along the protein are illustrated in Figure 2. Two bottleneck regions for the GLUT1 inward branch of the pathway and an extensive constricted zone in the outward branch of the pathway are observed. The key bottleneck residues defining each branch are shown in Figure 2. For simplicity, only bottleneck residues involved in more than 80 % of the snapshots analyzed are shown. From all the residues identified, a set of four create the main channel bottleneck observed in the inward-facing branch of the pathway in the gel state: R153, Q161, W388, and F389. Residues T30, I164, N288, and F291 define the bottleneck region of the outward branch. In the fluid phase, residues F26, N34, I168, Y292, S294 and T295 define the bottleneck region of the outward branch of the pathway, and residues P141, R153, H160, Q161, W388, and F389 the inward branch of the pathway. R153 is a key bottleneck residue for the inward branches of the pathways regardless of bilayer phase. However, its side chain position and interactions differ depending on the physical state of the bilayer. When GLUT1 is embedded in a fluid membrane, R153 forms a salt-bridge interaction with E243, which maintains both residues locked in a relatively stable conformation. In the gel phase, small conformational changes affecting the endofacial TM helix prevent formation of the R153-E245 salt bridge, resulting in a decrease of the tunnel width (Figure S5).

It is noteworthy that R153 is an absolutely conserved amino acid in the GLUT family, whereas F26, N34, P141, Q161, I164, I168, N288, Y292, and W388 are conserved in six or more GLUT members. Mutations of R153 and outward-facing T295 residues are related to glucose deficiency diseases (46, 47) and W388 has been shown to be critical for binding of ligands such as cytochalasin B and forskolin (48).

Analysis of the evolution of the size of the translocation pathway for glucose in GLUT1 described earlier, illustrates that in the gel phase the passage connecting the extracellular and intracellular sides of the GLUT1 transporter is closed. The inner regions of both the inward and outward branches of the permeation pathway are inaccessible. Under these circumstances, glucose transit via the inner branch of the GLUT1 pathway toward the central glucose binding site will be therefore be improbable. In contrast when the transporter is embedded in a lipid bilayer in the fluid phase *in silico* docking analysis shows that glucose can bind at any position along the permeation pathway, further confirming that passage across the transport via a staged diffusion process is a possible transit mechanism (Figure S7). These flexible structures corroborate the multisite model of sugar transport in the Xylem transporter based on multiple static crystal conformers (52). Experiments have demonstrated that ATP binding within this endofacial linker region, retards net glucose influx possibly by causing partial occlusion of the aperture shielding the internal transporter vestibule from the cytosolic solution (49).

To confirm that temperature effects on the transporter are not the cause for the change in size of the bottleneck radius, additional simulations were performed where the transporter and the lipid bilayer were coupled to independent thermostats set at different temperatures. In the simulation where the membrane is held at the gel phase temperature and the temperature of the GLUT1 transporter is raised above this temperature, both the inward- and outward branches of the tunnel still display the narrow bottleneck radius observed for GLUT1 embedded in a gel phase bilayer (Table S2).

Additionally, simulation of a GLUT1 transporter at a temperature below the gel phase temperature, embedded in a fluid membrane, displays open tunnels for the inward and outward branches. Together, these results eliminate protein

temperature as a principal modulator of the bottleneck radius and indicate that the force induced by the interaction with the membrane surface tension is critical to the size of the intramolecular voids that are crucial for the performance of the protein as a transmembrane transporter.

The results reveal a considerable similarity between the structural oscillations of the GLUT1 transporter in a fluid or gel membrane, although the latter restricts the magnitude of these movements. Comparison of the protein B-factors in the gel and fluid bilayers reveals an overall similarity of the thermal fluctuations of the residues in both gel and fluid phases, although these fluctuations are more constrained in the gel phase (Figure S7). In a fluid membrane the largest protein fluctuations occur in the linker regions between TM helices, especially in the endofacial domain. The gel phase reduces the global thermal fluctuations of the embedded protein in comparison to the fluid state, mainly affecting the C-terminal region of the transporter.

Although previously, membrane lipids were thought to play mainly a supportive role in biological transport processes, it has now become evident that they critically modulate protein function (50, 51). Here, several membrane properties were analyzed and compared in the fluid and gel phases, among these were the bilayer thickness, defined as the distance between the average positions of the head groups in the upper and lower leaflets. The average thickness of the membrane in the gel phase evolves over time to a higher value compared to the fluid membrane (42.5 vs 40 Å) (Figure S8A). This reflects a higher degree of order of the hydrophobic lipid tails in the gel phase. The computed values agree closely with those obtained from relative electron densities calculated through the bilayer normal of multi-lamellar dispersions of the phospholipids examined by synchrotron X-ray diffraction methods (gel, 42.4 Å; fluid, 40.2 Å; Figure S9). While a fluid membrane can accommodate the protein without alteration of the lipid structure, gel membranes are perturbed by the presence of the protein (Figure S8B). This is probably a consequence of the greater membrane thickness in the gel phase, due to denser lipid packing, and the interactions of the hydrophobic lipid tails and the transmembrane segments of the proteins. In order to further characterize the lipid structure in both phases, order

parameters for the lipids surrounding the protein and the bulk lipids were computed using the last 100 ns of the trajectories (Figure S8.D). Lipid tails in the gel phase show higher order parameters than in the fluid phase as expected, with lipids surrounding the protein displaying higher mobility. In the fluid phase, lipids show smaller order parameters and are not perturbed by the presence of the protein. The bilayer in which GLUT1 is interpolated at 35°C exhibited differences observed in bilayers of the pure lipid in the absence of the protein. Thus, while order parameters indicate the hydrocarbon chains are in a gel configuration, there is disorder of the chains at the protein-lipid interface. The characteristic tilt of the hydrocarbon chains with respect to the bilayer normal tend to a more vertical orientation and there is a variation in membrane thickness in the vicinity of the protein that is not consistent with a periodic ripple structure of the lipid.

To check whether the properties of the lipids in the external and cytoplasmic leaflets are affected differently by the presence of the protein average order parameters of the acyl chain and area/lipid were derived from the entire 400 ns and last 100 ns trajectories. The order parameters along the length of the chains were significantly greater in the external compared to the cytoplasmic leaflet in the respective gel and fluid phases throughout the simulations. This is consistent with calculated areas/lipid which were significantly less in the external compared to the cytoplasmic leaflet (See Table S2).

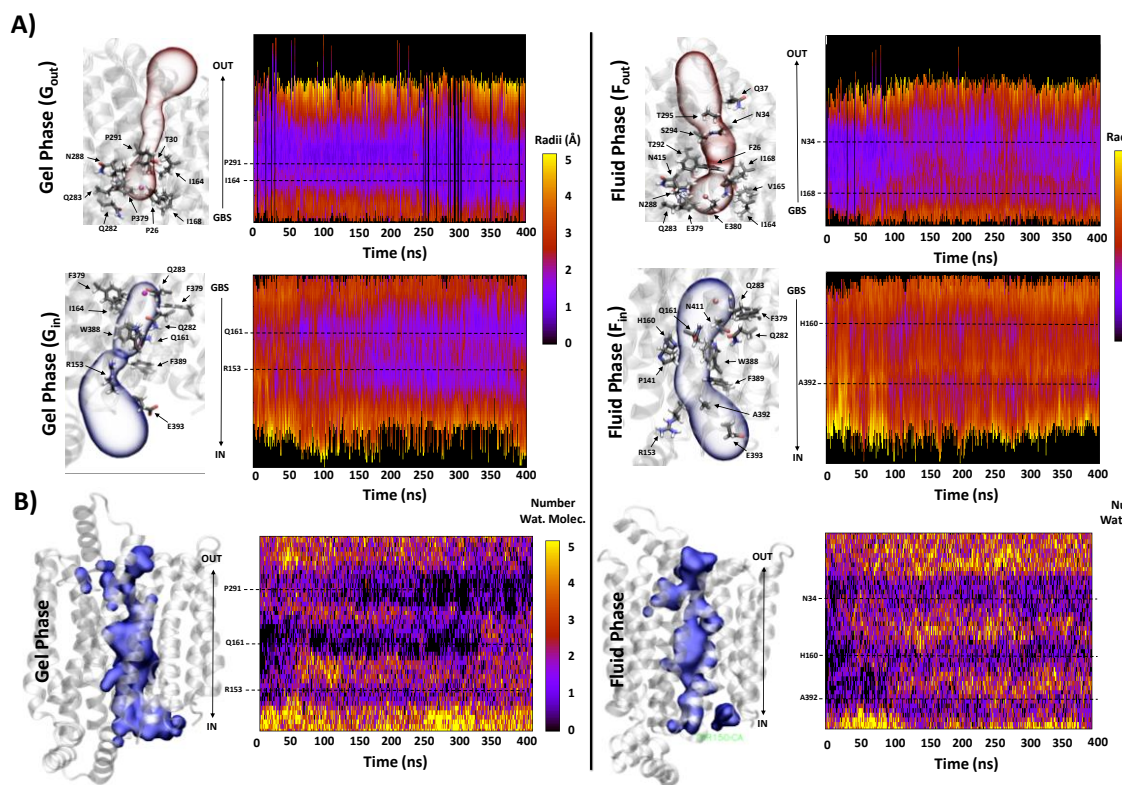


Figure 2. (A) Time evolution of the radius of the pathways for the F_{in} , F_{out} , G_{in} and G_{out} branches. The colour code reflects the width at each point in the pathway. Key bottleneck residues are indicated for each branch. F corresponds to the fluid phase and G to the gel phase. ‘In’ denotes the branch facing the intracellular side of the bilayer and ‘Out’ the extracellular side. (B) Time evolution of the number of water molecules within the GLUT1 channel. A continuous surface representation of the channel hydration for each GLUT1 MD trajectory is shown, where the tertiary structure of the transporter is shown in transparent representation.

As distinct from thermodynamic pressure of the system where any differences in pressure tend to zero, local differences in surface tension within the lipid bilayer arise as a result of the particular composition and phase state of the lipid where bilayer thickness, curvature and pressure profile generate differences in lateral pressure that constrain the area occupied by proteins interpolated into the bilayer (52). As a means of evaluating a possible correlation between the membrane phase and the bottleneck width, the membrane area and the bottleneck radius of the pathway were correlated (Figure S10.A). The correlation coefficient between the membrane area of the gel phase and the GLUT1 inward channel (G_{in}) was found to

be 0.66. This indicates that, for the Gin branch of the pathway, membrane areas exert sufficient pressure to compress the transporter, thereby, narrowing the GLUT1 inner pathway and impeding sugar transport (Figure 10.B). Similarly, by correlating the bottleneck radius with membrane thickness, a correlation coefficient of -0.54 for the Gin channel is obtained. This supports the view that only the gel phase of the membrane affects the dynamics of the transporter sufficiently to lead to occlusion of the channel, particularly in those regions located near the GLUT1 inward-face. In this case, the correlation indicates that an increase in the membrane thickness narrows GLUT1 C_{in} tunnel, probably by exerting a higher pressure onto the channel gate through the lipid head-groups, possibly aided by the observed distortions created within the bilayer plane. Clearly, these results lend further support to the view that the gel phase of the membrane influences the protein, leading to a narrower glucose translocation pathway that restricts glucose transport.

The degree of hydration of the protein has been studied as a channel with a radius of 1-2 Å contains some water under ambient conditions, and a change in the mean number of water molecules inside the protein or their distribution is likely to affect the accessibility of glucose. In this respect, the number and distribution of water molecules within the channel was computed over time (Figure S11) as well as the correlation between channel size and the number of water molecules, that is the degree of hydration. Water molecules freely diffuse along long sections of the main tunnel in the simulations where the lipid membrane is in fluid phase as compared to the gel phase. The main tunnel is interconnected by neighbouring segments whereas in the gel phase the connections do not extend across the entire channel due to compression of the protein at times.

The average numbers of water molecules existing within cavities along Z-axis of the central channel were subdivided into eight 5 Å wide zones in both gel and fluid phases were digitized and averaged during successive 300 ps intervals encompassing the entire 400 ns simulation time-course shown in Figure S11. The variations in water densities in each of the eight zones were correlated with the other seven, and a correlation map of all the regression coefficients obtained for the gel and fluid phase waters. The findings indicate that water freely diffuses along longer tunnel

segments in the fluid phase than in the gel phase. In the fluid phase the entire channel length is connected by neighbouring high correlated segments. In contrast, in the gel phase, the regions of high connectivity are interrupted due to longer closure times in the bottleneck regions. This segmentation can be ascribed to external compression exerted by gel membrane. In the gel phase it is apparent that water from the central zones is displaced toward expanded external vestibules, so there is relatively little net change in the total number of water molecules within the central channel regions as a result of compression of the transporter due to compression.

It is evident from the dynamics of number of water molecules occupying the central channel that there are three bottleneck positions with two intermediate cavities. The upper two bottlenecks appear to be more temperature sensitive than the lowest (internal) bottleneck. The gel-fluid phase transformation will result in a much higher percentage closure time of the bottlenecks to water and presumably to glucose. The reduced temperature effect transforms the interpretation with regard to the mechanism of glucose transport.

The alternating access model proposes one choke point in the transport process here we have a series of three. The effect of cooling is normally interpreted as being due to slowing of the rate processes of the transporter inversions. Here it is evident that cooling results mainly in narrowing of the channel particularly at the bottlenecks. Thus slowing of transport is consistent with reduced rates of staged diffusion, as is consistent with the model proposed recently in (40).

It is important to recognize that this work only covers a symmetrical DPPC membrane, whereas lipid organization in the human plasma membrane is asymmetric and highly heterogeneous. Therefore, much more complex interactions can be expected. In this regard, a recent article by Hresko *et al.* (59) highlighted the activation effect of anionic phospholipids on the turnover rate of GLUT3 and GLUT4 transporters, while the substrate affinity remained unaltered, providing evidence of a direct interaction of the studied phospholipids with the transporter. Anionic phospholipids are found exclusively on the endofacial leaflet of mammalian lipid

bilayers, thus, supporting a crucial role for bilayer composition on transporter activity.

The extent that membrane phase alters glucose diffusion through the central channel awaits further simulations. The role of the more salient single point mutations within the channel also awaits investigation.

Conclusions

MD simulations of the GLUT1 transporter embedded in a gel or fluid DPPC membrane bilayer have been performed to study the effects of the bilayer physical state on the dimensions and dynamics of the glucose translocation pathways within GLUT1. Hydrated DPPC bilayers form gel phases at temperatures between lamellar crystal phases ($<7^{\circ}\text{C}$) and lamellar liquid-crystal phase ($>41^{\circ}\text{C}$). Here, we have demonstrated that the presence of GLUT1 causes a disturbance of the bilayer structure at temperatures where a gel phase of the pure phospholipid is observed. The gel phase of DPPC has been well characterized by a range of biophysical techniques including X-ray diffraction (data used to prepare Fig S8) and MD simulations (53). Here, inhomogeneity of the lipids is observed in the vicinity of GLUT1 due to the protein. When embedded in a fluid membrane as opposed to in a gel phase, GLUT1 exhibited a larger bottleneck radius for both, the main endofacial and exofacial branches of the primary pathway connecting the extracellular and intracellular sides of the bilayer. The external branch of the pathway in the fluid phase was found principally closed, with bottleneck values smaller than the minimal glucose radius. However, transient open conformations that could allow glucose passage were also detected. Overall, these results confirm the viability of a multi-site model for glucose translocation where sugar molecules diffuse through a network of binding sites whilst the overall global conformation of the protein is conserved. Although the differences in diameter observed in the simulation are small, nevertheless our contention that this is a factor limiting passage through the channel is not unreasonable. This is consistent with the report by Fu *et al.* (45) showing that unhydrated glucose can negotiate the narrowest dimensions of the channel by spontaneous diffusion.

Author Contributions. JIF and CD performed the simulations and analyzed the data. JFI, PJQ., RN and C.D. planned the simulations, interpreted the data and wrote the manuscript.

Acknowledgements. ARCHER, the UK National Supercomputing Service (<http://www.archer.ac.uk>), the Hartree Center, and the National Service for Computational Chemistry Software are acknowledged for providing computational resources. This work was supported by the Biotechnology and Biological Sciences Research Council (BB/L01825X/1).

References

1. Pao, S. S., I. T. Paulsen, and M. H. Saier. 1998. Major facilitator superfamily. *Microbiol Mol Biol R* 62:1-+.
2. Manolescu, A. R., K. Witkowska, A. Kinnaird, T. Cessford, and C. Cheeseman. 2007. Facilitated hexose transporters: New perspectives on form and function. *Physiology* 22:234-240.
3. Mueckler, M., and B. Thorens. 2013. The SLC2 (GLUT) family of membrane transporters. *Mol Aspects Med* 34:121-138.
4. Zhao, F. Q., and A. F. Keating. 2007. Functional properties and genomics of glucose transporters. *Curr Genomics* 8:113-128.
5. Deng, D., and N. Yan. 2016. GLUT, SGLT, and SWEET: Structural and mechanistic investigations of the glucose transporters. *Protein science : a publication of the Protein Society* 25:546-558.
6. Robichaud, T., A. N. Appleyard, R. B. Herbert, P. J. F. Henderson, and A. Carruthers. 2011. Determinants of Ligand Binding Affinity and Cooperativity at the GLUT1 Endofacial Site. *Biochemistry* 50:3137-3148.
7. De Zutter, J. K., K. B. Levine, D. Deng, and A. Carruthers. 2013. Sequence Determinants of GLUT1 Oligomerization ANALYSIS BY HOMOLOGY-SCANNING MUTAGENESIS. *Journal of Biological Chemistry* 288:20734-20744.
8. Carruthers, A., J. DeZutter, A. Ganguly, and S. U. Devaskar. 2009. Will the original glucose transporter isoform please stand up! *Am J Physiol-Endoc M* 297:E836-E848.
9. Zhao, Y., D. Terry, L. Shi, H. Weinstein, S. C. Blanchard, and J. A. Javitch. 2010. Single-molecule dynamics of gating in a neurotransmitter transporter homologue. *Nature* 465:188-193.
10. Liu, Y., M. Ke, and H. Gong. 2015. Protonation of Glu(135) Facilitates the Outward-to-Inward Structural Transition of Fucose Transporter. *Biophys J* 109:542-551.
11. Deng, D., C. Xu, P. C. Sun, J. P. Wu, C. Y. Yan, M. X. Hu, and N. Yan. 2014. Crystal structure of the human glucose transporter GLUT1. *Nature* 510:121-+.
12. Nomura, S., S. Sakamaki, M. Hongu, E. Kawanishi, Y. Koga, T. Sakamoto, Y. Yamamoto, K. Ueta, H. Kimata, K. Nakayama, and M. Tsuda-Tsukimoto. 2010. Discovery of Canagliflozin, a Novel C-Glucoside with Thiophene Ring, as Sodium-Dependent Glucose Cotransporter 2 Inhibitor for the Treatment of Type 2 Diabetes Mellitus. *Journal of medicinal chemistry* 53:6355-6360.
13. Deng, D., P. C. Sun, C. Y. Yan, M. Ke, X. Jiang, L. Xiong, W. L. Ren, K. Hirata, M. Yamamoto, S. L. Fan, and N. Yan. 2015. Molecular basis of ligand recognition and transport by glucose transporters. *Nature* 526:391-+.

14. Quistgaard, E. M., C. Low, F. Guettou, and P. Nordlund. 2016. Understanding transport by the major facilitator superfamily (MFS): structures pave the way. *Nature reviews. Molecular cell biology*.
15. Cunningham, P., I. Afzal-Ahmed, and R. J. Naftalin. 2006. Docking studies show that D-glucose and quercetin slide through the transporter GLUT1. *Journal of Biological Chemistry* 281:5797-5803.
16. Cunningham, P., and R. J. Naftalin. 2013. Implications of Aberrant Temperature-Sensitive Glucose Transport Via the Glucose Transporter Deficiency Mutant (GLUT1DS) T295M for the Alternate-Access and Fixed-Site Transport Models. *J Membrane Biol* 246:495-511.
17. Naftalin, R. J. 2008. Osmotic water transport with glucose in GLUT2 and SGLT. *Biophysical Journal* 94:3912-3923.
18. Fu, X. G., G. Zhang, R. Liu, J. Wei, D. Zhang-Negrerie, X. D. Jian, and Q. Z. Gao. 2016. Mechanistic Study of Human Glucose Transport Mediated by GLUT1. *Journal of Chemical Information and Modeling* 56:517-526.
19. Saita, E., D. Albanesi, and D. de Mendoza. 2016. Sensing membrane thickness: Lessons learned from cold stress. *Biochimica et Biophysica Acta (BBA) - Molecular and Cell Biology of Lipids* 1861:837-846.
20. Cybulski, L. E., M. Martín, M. C. Mansilla, A. Fernández, and D. de Mendoza. 2010. Membrane Thickness Cue for Cold Sensing in a Bacterium. *Current Biology* 20:1539-1544.
21. Connolly, T. J., A. Carruthers, and D. L. Melchior. 1985. Effects of Bilayer Cholesterol on Human-Erythrocyte Hexose-Transport Protein-Activity in Synthetic Lecithin Bilayers. *Biochemistry* 24:2865-2873.
22. Tefft, R. E., A. Carruthers, and D. L. Melchior. 1986. Reconstituted Human-Erythrocyte Sugar Transporter Activity Is Determined by Bilayer Lipid Head Groups. *Biochemistry* 25:3709-3718.
23. Carruthers, A., and D. L. Melchior. 1984. Human-Erythrocyte Hexose Transporter Activity Is Governed by Bilayer Lipid-Composition in Reconstituted Vesicles. *Biochemistry* 23:6901-6911.
24. Yuli, I., W. Wilbrandt, and M. Shinitzky. 1981. Glucose transport through cell membranes of modified lipid fluidity. *Biochemistry* 20:4250-4256.
25. Jo, S., T. Kim, and W. Im. 2007. Automated Builder and Database of Protein/Membrane Complexes for Molecular Dynamics Simulations. *PloS one* 2.
26. Jo, S., T. Kim, V. G. Iyer, and W. Im. 2008. Software news and updates - CHARNIM-GUI: A web-based graphical user interface for CHARMM. *Journal of computational chemistry* 29:1859-1865.
27. Phillips, J. C., R. Braun, W. Wang, J. Gumbart, E. Tajkhorshid, E. Villa, C. Chipot, R. D. Skeel, L. Kale, and K. Schulten. 2005. Scalable molecular dynamics with NAMD. *J Comput Chem* 26:1781-1802.
28. Klauda, J. B., R. M. Venable, J. A. Freites, J. W. O'Connor, D. J. Tobias, C. Mondragon-Ramirez, I. Vorobyov, A. D. MacKerell, and R. W. Pastor. 2010. Update of the CHARMM All-Atom Additive Force Field for Lipids: Validation on Six Lipid Types. *J Phys Chem B* 114:7830-7843.
29. MacKerell, A. D., D. Bashford, M. Bellott, R. L. Dunbrack, J. D. Evanseck, M. J. Field, S. Fischer, J. Gao, H. Guo, S. Ha, D. Joseph-McCarthy, L. Kuchnir, K. Kuczera, F. T. K. Lau, C. Mattos, S. Michnick, T. Ngo, D. T. Nguyen, B. Prodhom, W. E. Reiher, B. Roux, M. Schlenkrich, J. C. Smith, R. Stote, J. Straub, M. Watanabe, J. Wiorkiewicz-Kuczera, D. Yin, and M. Karplus. 1998. All-atom empirical potential for molecular modeling and dynamics studies of proteins. *Journal of Physical Chemistry B* 102:3586-3616.

30. Jorgensen, W. L., J. Chandrasekhar, J. D. Madura, R. W. Impey, and M. L. Klein. 1983. Comparison of Simple Potential Functions for Simulating Liquid Water. *Journal of Chemical Physics* 79:926-935.
31. Feller, S. E., Y. H. Zhang, R. W. Pastor, and B. R. Brooks. 1995. Constant-Pressure Molecular-Dynamics Simulation - the Langevin Piston Method. *Journal of Chemical Physics* 103:4613-4621.
32. Darden, T., D. York, and L. Pedersen. 1993. Particle Mesh Ewald - an N.Log(N) Method for Ewald Sums in Large Systems. *J Chem Phys* 98:10089-10092.
33. Verlet, L. 1967. Computer Experiments on Classical Fluids .I. Thermodynamical Properties of Lennard-Jones Molecules. *Phys Rev* 159:98-&.
34. Miyamoto, S., and P. A. Kollman. 1992. SETTLE - an analytical version of the Shake and Rattle algorithm for rigid water models. *Journal of computational chemistry* 13:952-962.
35. Tuckerman, M., B. J. Berne, and G. J. Martyna. 1992. Reversible Multiple Time Scale Molecular-Dynamics. *Journal of Chemical Physics* 97:1990-2001.
36. Abraham, M. J., T. Murtola, R. Schulz, S. Páll, J. C. Smith, B. Hess, and E. Lindahl. 2015. GROMACS: High performance molecular simulations through multi-level parallelism from laptops to supercomputers. *SoftwareX* 1–2:19-25.
37. Chovancova, E., A. Pavelka, P. Benes, O. Strnad, J. Brezovsky, B. Kozlikova, A. Gora, V. Sustr, M. Klvana, P. Medek, L. Biedermannova, J. Sochor, and J. Damborsky. 2012. CAVER 3.0: A Tool for the Analysis of Transport Pathways in Dynamic Protein Structures. *Plos Computational Biology* 8.
38. Guixa-Gonzalez, R., I. Rodriguez-Espigares, J. M. Ramirez-Anguita, P. Carrio-Gaspar, H. Martinez-Seara, T. Giorgino, and J. Selent. 2014. Membplugin: Studying Membrane Complexity in Vmd. *Bioinformatics* 30:1478-1480.
39. Morris, G. M., R. Huey, W. Lindstrom, M. F. Sanner, R. K. Belew, D. S. Goodsell, and A. J. Olson. 2009. AutoDock4 and AutoDockTools4: Automated Docking with Selective Receptor Flexibility. *J Comput Chem* 30:2785-2791.
40. Cunningham, P., and R. J. Naftalin. 2014. Reptation-Induced Coalescence of Tunnels and Cavities in Escherichia Coli Xyle Transporter Conformers Accounts for Facilitated Diffusion. *J Membrane Biol* 247:1161-1179.
41. Barnett, C. B., and K. J. Naidoo. 2010. Ring Puckering: A Metric for Evaluating the Accuracy of AM1, PM3, PM3CARB-1, and SCC-DFTB Carbohydrate QM/MM Simulations. *Journal of Physical Chemistry B* 114:17142-17154.
42. Naftalin, R. J. 2008. Alternating carrier models of asymmetric glucose transport violate the energy conservation laws. *Biophys J* 95:4300-4314.
43. Carruthers, A., J. DeZutter, A. Ganguly, and S. U. Devaskar. 2009. Will the original glucose transporter isoform please stand up! *Am J Physiol Endocrinol Metab* 297:E836-848.
44. Cunningham, P., and R. J. Naftalin. 2014. Reptation-induced coalescence of tunnels and cavities in Escherichia Coli Xyle transporter conformers accounts for facilitated diffusion. *J Membr Biol* 247:1161-1179.
45. Fu, X., G. Zhang, R. Liu, J. Wei, D. Zhang-Negrerie, X. Jian, and Q. Gao. 2016. Mechanistic Study of Human Glucose Transport Mediated by GLUT1. *J Chem Inf Model* 56:517-526.
46. Klepper, J., and T. Voit. 2002. Facilitated glucose transporter protein type 1 (GLUT1) deficiency syndrome: impaired glucose transport into brain - a review. *Eur J Pediatr* 161:295-304.
47. Klepper, J., and B. Leiendecker. 2007. GLUT1 deficiency syndrome - 2007 update. *Dev Med Child Neurol* 49:707-716.

48. Garcia, J. C., M. Strube, K. Leingang, K. Keller, and M. M. Mueckler. 1992. Amino-Acid Substitutions at Tryptophan-388 and Tryptophan-412 of the Hepg2 (Glut1) Glucose Transporter Inhibit Transport Activity and Targeting to the Plasma-Membrane in *Xenopus* Oocytes. *Journal of Biological Chemistry* 267:7770-7776.
49. Leitch, J. M., and A. Carruthers. 2007. ATP-dependent sugar transport complexity in human erythrocytes. *American Journal of Physiology - Cell Physiology* 292:C974-C986.
50. Dacosta, C. J. B., L. Dey, J. P. D. Therien, and J. E. Baenziger. 2013. A distinct mechanism for activating uncoupled nicotinic acetylcholine receptors. *Nature Chemical Biology* 9:701-+.
51. Sadiq, S. K., R. Guixa-Gonzalez, E. Dainese, M. Pastor, G. De Fabritiis, and J. Selent. 2013. Molecular Modeling and Simulation of Membrane Lipid-Mediated Effects on GPCRs. *Curr Med Chem* 20:22-38.
52. Battle, A. R., P. Ridone, N. Bavi, Y. Nakayama, Y. A. Nikolaev, and B. Martinac. 2015. Lipid-protein interactions: Lessons learned from stress. *Biochimica et Biophysica Acta (BBA) - Biomembranes* 1848:1744-1756.
53. Redmill, P. S., and C. McCabe. 2010. A Molecular Dynamics Study of the Behavior of Selected Nanoscale Building Blocks in a Gel-Phase Lipid Bilayer. *The journal of physical chemistry. B* 114:9165-9172.